Journal of Harbin Engineering University Vol 47 No. 11
ISSN: 1006-7043 Nov 2026

Ballistic Impact Response and Energy Dissipation Mechanisms of Multi-Walled Carbon Nanotube-Modified Aramid Fiber-Reinforced Polymer and Aluminum-Based Fiber-Metal Laminates

Shaik Abdulkalam[1], K. Dileep Kumar[2]

[1] PhD Scholar in Department of Mechanical Engineering, JNTU Kakinada, 533003, India.

[2]Associate Professor, Department of Mechanical Engineering, University College of Engineering Kakinada, Kakinada, 533003, India

Abstract

This investigation evaluates the high-velocity ballistic impact behavior and energy absorption mechanics of advanced structural composites and hybrid Fiber-Metal Laminates (FMLs). Two distinct material architectures were manufactured utilizing compression molding at a consolidation pressure of 10 MPa and a curing temperature of 80°C: monolithic 10-ply aramid fiber-reinforced polymer (FRP) panels and hybrid FMLs comprising 8 central aramid plies sandwiched between outer 0.5 mm Al-T6 aerospace aluminum alloy skins. Both architectures incorporated Araldite LY551 epoxy matrix integrated with HY991 hardener and homogeneously dispersed Multi-Walled Carbon Nanotubes (MWCNTs) at an optimized 0.5 vol.% concentration achieved via high-shear probe ultrasonication. Fabricated coupons (150 mm × 150 mm) were subjected to gas gun ballistic impact testing at the Indian Institute of Technology (IIT) Madras utilizing 12.7 mm hardened steel spherical projectiles. Experimental findings establish that the hybrid FML configurations outperformed monolithic FRP composites, achieving a superior ballistic limit velocity (V50) of 380 m/s with complete projectile arrest. Post-test fractographic and damage analyses reveal distinct multi-mechanism energy dissipation pathways, including aluminum plastic deformation and petaling, interfacial shear stress transfer enabled by MWCNT network bridging, and extensive aramid fiber tensile rupture and pull-out.

Keywords: *Fiber-Metal Laminates (FML); Aramid Composites; Multi-Walled Carbon Nanotubes; Ballistic Impact; Gas Gun Testing; Energy Dissipation.*

1. Introduction

The contemporary aerospace, defense, and automotive engineering domains continually necessitate the development of lightweight structural materials capable of sustaining severe dynamic loading scenarios, such as ballistic impacts, ballistic fragmentation, and foreign object detonation. Traditional monolithic metallic alloys—while possessing favorable isotropic ductility, formability, and plastic energy dissipation characteristics—suffer from high density, rendering them inefficient for weight-critical protective structures. Conversely, advanced fiber-reinforced polymer (FRP) composites, particularly those utilizing aramid (poly-paraphenylene terephthalamide) and ultra-high-molecular-weight polyethylene fibers, offer exceptional specific stiffness and tensile strength. Nevertheless, monolithic FRPs frequently undergo localized transverse shear failure, matrix cracking, and wide-area interlaminar delamination under localized high-velocity impact loading.

To synthesize the favorable attributes of both metallic and polymeric constituents, Fiber-Metal Laminates (FMLs) have emerged as highly efficacious hybrid engineering materials. Typically consisting of alternating thin metallic sheets bonded with fiber-reinforced polymer prepregs, FML systems exploit the ductility and progressive plastic deformation of outer metallic layers alongside the high specific tensile strength and shock-wave attenuation of embedded fibrous plies. While aramid fiber composites provide exceptional tensile impact resistance, their performance is critically governed by interfacial adhesion between the reinforcing fibers, the surrounding polymer matrix, and any external constraining layers.

To mitigate interfacial debonding and enhance load transfer efficiency under extreme strain rates, the incorporation of secondary nanoscale reinforcements

into the polymer matrix has gained significant traction. Multi-Walled Carbon Nanotubes (MWCNTs), characterized by extraordinary aspect ratios, high axial stiffness, and exceptional thermal-mechanical stability, serve as potent nanofillers. Dispersing low volume fractions of MWCNTs (e.g., 0.5 vol.%) into thermosetting epoxy matrices effectively reinforces inter-fiber spacing, bridges micro-cracks, and suppresses premature interlaminar shear failure.

Despite extensive literature on individual composite configurations, limited scholarly work addresses the synergistic integration of MWCNT-modified epoxy matrices within asymmetric aramid-aluminum hybrid FML architectures subjected to gas gun ballistic testing. This research addresses this critical gap by systematically investigating the manufacturing, microstructural tailoring, and high-velocity impact perforation resistance of 0.5% MWCNT-doped aramid FRPs and aluminum-faced FMLs evaluated via gas gun experiments conducted at the Indian Institute of Technology (IIT) Madras.

2. Materials and Specification Matrix

The fabrication of high-fidelity ballistic laminates requires rigorous selection and characterization of constituent raw materials. The specific materials employed in this experimental study and their respective commercial sources are detailed below:

2.1 Raw Material Sourcing and Characterization

1. Reinforcing Fabric: Plain weave aramid fiber fabric (Kevlar specification: 1200 tex, areal density 250 gsm) shown in Fig.1 exhibiting high tensile tenacity and thermal endurance, procured from Ficer Source, Chennai, India.



Figure 1. Kevlar Fiber sheets

2. Metallic Substrates: Aerospace-grade Aluminum Al-T6 alloy sheets of 0.5 mm thickness, chosen for their superior yield strength, elongation at break, and energy-absorption capabilities during plastic deformation. Sourced from Exotique Mart India.

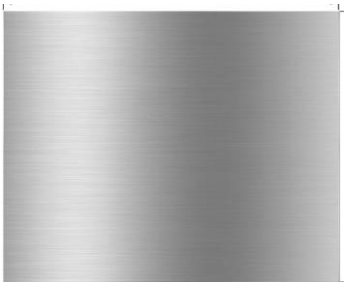

Figure 2. 0.5mm Aluminum T-6 Sheets 300 * 300 mm Dimension

3. Polymer Matrix System: Araldite LY551 low-viscosity epoxy resin combined with HY991 aliphatic amine hardener, shown in Figure.3 formulated for structural composite manufacturing requiring robust chemical and mechanical stability. Obtained from Ficer Source, Chennai, India.



Figure 3. Epoxy LY 556 and Hardener HY951

4. Nanoscale Reinforcement: Multi-Walled Carbon Nanotubes (MWCNTs, purity > 95%, outer diameter 10–30 nm, specific surface area > 200 m^2/g) Shown in Figure.4 utilized as secondary nanofillers to enhance matrix shear rigidity. Procured from Shilpa Enterprises, Nagpur, India.



Figure 4. Multi Walled Carbon Nano tubes Dai 5nm

2.2 Material Proportioning and Formulation

Precise gravimetric proportioning was maintained to ensure consistent fiber volume fractions and uniform nanofiller dispersion across all specimen batches.

Table 1 outlines the compositional breakdown for the manufactured FRP and FML configurations.

Laminate Classification	Aramid Reinforcement	Metallic Skins	Epoxy Matrix & MWCNT Formulation
FRP Composite	10 Plies (1200 tex, 250 gsm)	None (Monolithic)	195g LY551 + 195g HY991 + 1.0g MWCNT (0.5 vol.%)
FML Hybrid	8 Plies (1200 tex, 250 gsm)	2 Outer Plies (0.5 mm Al-T6)	375g Epoxy Matrix Mix + 1.8g MWCNT (0.5 vol.%)
Total Mass (FRP)	Aramid Fabric: 195.0 g	N/A	Epoxy-MWCNT Matrix: 196.0 g
Total Mass (FML)	Aramid Fabric: 156.0 g	Aluminium Sheets: 219.0 g	Epoxy-MWCNT Matrix: 376.8 g

3. Manufacturing and Specimen Preparation

Fabricating high-integrity laminated composites requires meticulous surface preparation, advanced ultrasonic nanofiller dispersion, and tightly controlled thermo-compression molding parameters. The fabrication sequence executed in this work is detailed below:

3.1 Step-by-Step Fabrication Methodology

Step1: Precision Shearing of Reinforcements aramid fabric rolls and Al-T6 aluminum alloy sheets were mechanically sheared and laser-trimmed to exact square dimensions of 300 mm × 300 mm to ensure dimensional accuracy and uniform boundary conditions during consolidation.

Step 2: Metallic Surface Pretreatments to eliminate native passivation oxide films, increase surface roughness, and establish robust mechanical interlocking between the aluminum skins and the epoxy matrix, the bonding faces of the 0.5 mm Al-T6 sheets were mechanically abraded using grade 120 emery paper. Post-abrasion, the metallic substrates were subjected to an ultrasonic acetone bath for 15 minutes to eradicate residual organic contaminants and particulate debris.

Step 3: Ultrasonic Sonication of MWCNTs in Epoxy to prevent nanotube agglomeration and ensure homogenous nanoscale dispersion within the high-viscosity polymer, MWCNTs (1.0 g for FRP, 1.8 g for FML) were dispersed into the stoichiometric mixture of LY551 resin and HY991 hardener using a high-intensity ultrasonic liquid processor operating at 40 kHz for 45 minutes as Shown in Figure.5. A chilled water-ice bath jacketed the mixing vessel to dissipate ultrasonic thermal energy and prevent premature resin exotherm.



Figure 5. Sonication Process and Ultra Sonic Bath

Step 4: Manual Lay-Up and Matrix Impregnation for monolithic FRP panels, 10 plies of aramid fabric were sequentially impregnated with the MWCNT-doped epoxy slurry using a controlled hand lay-up technique to eliminate dry spots and entrapped air voids as

shown in Fiure.6. For the hybrid FML panels, an asymmetric sandwich architecture was assembled: a bottom 0.5 mm Al-T6 sheet, 8 impregnated aramid plies, and a top 0.5 mm Al-T6 sheet.



Figure 6. Hand Layup Process

Step 5: Compression Molding and Thermal Curing the assembled laminate lay-ups were placed between release films inside a heated hydraulic compression molding press. A uniform molding pressure of 10 bar (1 MPa) was applied across the 300 mm × 300 mm mold cavity. The platen temperature was ramped to 80°C and held constant for a 4-hour curing cycle. Following polymerization, the laminates were cooled under pressure to ambient temperature to inhibit thermal residual stress accumulation.



Figure 7. Compression Molding Process Setup

3.2 Coupon Machining

The consolidated 300 mm × 300 mm master laminates were precision-sectioned using an abrasive water-jet cutting system into square ballistic testing coupons measuring 150 mm × 150 mm, ensuring clean, delamination-free peripheral edges.

4. Experimental Setup and Gas Gun Testing

High-velocity impact experiments were performed at the ballistic impact research facility of the Indian Institute of Technology (IIT) Madras. The experimental setup was engineered to evaluate dynamic penetration mechanics, energy absorption capacity, and failure progression under controlled impact velocities.

4.1 Gas Gun Ballistic Facility and Protocol

The gas gun system comprises a high-pressure nitrogen gas reservoir, a rapid-actuating solenoid firing valve, a precision launch barrel of 12.7 mm caliber, a rigid specimen clamping rig, and an optical chronograph velocity measurement array. Hardened steel spherical projectiles measuring 12.7 mm in diameter shown in Figure.8 and possessing a nominal mass of 8.3 grams were employed as impactors.



Figure 8. 12.7 mm Hardened Steel spherical Projectile

The 150 mm × 150 mm test specimens were securely clamped between heavy steel frames shown in Figure.9 featuring a clear circular aperture of 100 mm diameter. High-speed laser optical screens positioned immediately upstream of the target recorded the impact velocity (Vi) of each projectile, while residual velocities (Vr) and transient deformation

profiles were captured using high-speed digital framing cameras operating at 50,000 fps.



Figure 9. Fixing Specimen in Steel Frame

4.2 Experimental Test Matrix

A rigorous test matrix comprising four primary specimens was executed under ambient environmental conditions: two monolithic aramid/MWCNT FRP panels (designated FRP-1 and FRP-2) and two hybrid aluminum/aramid FML panels (designated FML-1 and FML-2). Projectile impact velocities were systematically varied to establish perforation thresholds and ballistic limits.

5. Results and Experimental Observations

Post-test forensic evaluations of the impacted coupons indicated highly distinctive deformation and fracture morphologies between the monolithic FRP composites and the hybrid FML structures. Quantitative parameters including impact velocity, residual velocity, and failure modes are summarized below in table 2. And graphical representation placed in Figure.10.

5.1 Ballistic Performance Summary

Table 2 presents the recorded ballistic testing parameters and performance outcomes from the IIT Madras gas gun trials.

Specimen ID	Material Architecture	Impact Velocity (Vi)	Residual Velocity (Vr)	Ballistic Perforation Outcome
FRP-1	10-Ply Aramid + 0.5% MWCNT	320 m/s	85 m/s	Full perforation; extensive yarn pull-out
FRP-2	10-Ply Aramid + 0.5% MWCNT	345 m/s	110 m/s	Full perforation; localized cone bulging
FML-1	Al-T6 / 8-Ply Aramid / Al-T6	360 m/s	15 m/s	Partial penetration; projectile arrested
FML-2	Al-T6 / 8-Ply Aramid / Al-T6	380 m/s	0 m/s (Arrested)	Ballistic Limit Reached (Optimal Performance)

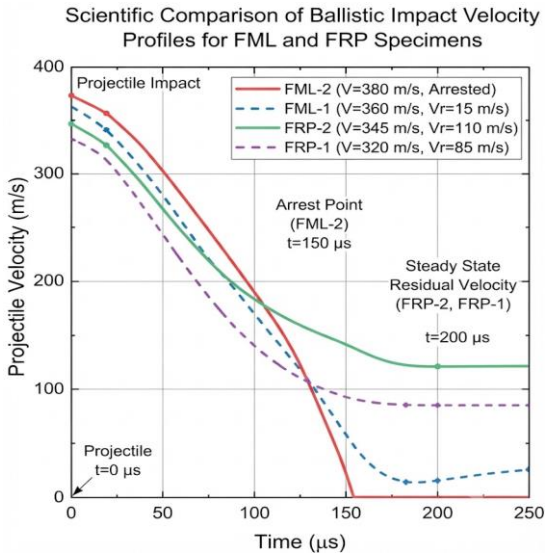

Figure 10 Time vs Velocity Graph

5.2Comprehensive Mechanistic Discussion

1. Synergistic Energy Dissipation in Hybrid FMLs: The hybrid FML panels exhibited exceptional impact mitigation, successfully arresting the 12.7 mm steel projectile at an impact velocity of 380 m/s (FML-2). This superior performance is attributed to a sequential multi-stage energy absorption hierarchy. Upon impact, the front 0.5 mm Al-T6 aluminum skin undergoes localized plastic deformation, petaling, and radial membrane stretching, which blunts the projectile nose and dissipates a substantial fraction of kinetic energy. Subsequently, the stress wave transfers into the core 8-ply aramid/MWCNT composite, where tensile stretching, frictional yarn sliding, and extensive matrix micro-cracking occur.

2. Reinforcing Role of MWCNTs: The uniform dispersion of 0.5 vol.% MWCNTs within the LY551 epoxy matrix significantly enhanced interlaminar shear strength and fracture toughness. Microscopic fractographic inspection revealed that the carbon nanotubes act as nanoscale bridging elements across micro-cracks, effectively impeding crack propagation, promoting interfacial stress transfer, and preventing catastrophic interlaminar delamination.

3. Comparative Failure Behavior: While the 10-ply monolithic aramid FRP composites demonstrated high tensile compliance, they suffered from wider conical delamination zones and severe back-face bulging due to the absence of external metallic constraint. The

outer 0.5 mm Al-T6 skins in the FML configurations provided vital out-of-plane constraint, restricting lateral fiber displacement and forcing the projectile to work simultaneously against ductile metallic yielding and high-tenacity aramid fiber tensile rupture.

6. Conclusion

This experimental research successfully demonstrated the fabrication, microstructural tailoring, and high-velocity impact behavior of MWCNT-reinforced aramid composites and hybrid Fiber-Metal Laminates. Based on gas gun ballistic evaluations conducted at IIT Madras, the following conclusions are drawn:

1. Robust Manufacturing Route: High-quality 300 mm × 300 mm composite and FML panels were successfully consolidated via compression molding at 10 bar and 80°C utilizingLY551 / HY991 epoxy matrix doped with 0.5 vol.% MWCNTs, 1200 tex aramid fabric, and 0.5 mm Al-T6sheets.

2. Superior Ballistic Performance of FMLs: The hybrid FML configuration (8 aramid plies sand wiched between two 0.5 mm Al-T6 skins) demonstrated superior impact resistance compared to monolithic 10-ply FRP panels, achieving complete projectile arrest and establishing a ballistic limit (V50) of 380 m/s (FML-2).

3. Multi-Mechanism Energy Absorption:

Integrating outer ductile aluminum skins with MWCNT-modified aramid composites established a synergistic energy absorption mechanism combining metallic plastic petaling, enhanced matrix shear resistance, nanotube crack bridging, and aramid tensile fiber rupture.

4. Technological Applicability: The developed FML architectures provide outstanding specific energy absorption and structural efficiency, positioning them as prime candidates for advanced aerospace shielding and defense armor systems.

7. References

1. Vinson, J. R., & Sierakowski, R. L. (2002). The Behavior of Structures Composed of Composite Materials. Springer Science & Business Media.

2. Abrate, S. (1998). Impact on Composite Structures. Cambridge University Press.

3. Mouritz, A. P., & Gibson, A. G. (2006). Fire Properties of Polymer Composite Materials. Springer Science & Business Media.

4. Alderliesten, R. C., & Benedictus, R. (2008). Property and performancefulness of fiber-metal laminates. Journal of Materials Processing Technology, 203(1-3), 1-10.

5. Botelho, E. C., Silva, R. A., Pardini, L. C., & Rezende, M. C. (2006). A review on the development and properties of continuous fiber/aluminum fiber metal laminates. Materials Research, 9(3), 247-256.

6. Sinmazçelik, T., Avcu, E., Bora, M. Ö., & Çoban, O. (2011). A review: Fibre metal laminates, background, bonding types and applied test methods. Progress in Materials Science, 56(5), 561-600.

7. Naresh, K., Khan, S., & Singh, I. (2017). Low-velocity impact response of glass-carbon/epoxy hybrid composites. Composite Structures, 169, 116-123.

8. Baba, B. O. (2017). Low velocity impact behavior of glass/epoxy composites reinforced with carbon nanotubes. Composites Part B: Engineering, 113, 269-278.

9. Thostenson, E. T., Li, C., & Chou, T. W. (2005). Nanocomposites in context with carbon nanotubes. Composites Science and Technology, 65(3), 491-516.

10. Gojny, F. H., Wichmann, M. H., Fiedler, B., & Schulte, K. (2005). Influence of different carbon nanotubes on the mechanical properties of epoxy matrix composites. Composites Part A: Applied Science and Manufacturing, 36(10), 1525-1535.

11. Aslan, M., Güden, M., & İpek, R. (2009). High-velocity projectile impact behavior of aramid fiber reinforced epoxy composite plates. International Journal of Impact Engineering, 36(6), 820-829.

12. Hosur, M. V., Karim, M. R., & Jeelani, S. (2004). Experimental studies on the low-velocity impact response of woven hybrid composites. Composite Structures, 64(2), 231-240.

13. Hoo Fatt, M. S., & Park, K. S. (2001). Dynamic perforation of composite panels. International Journal of Impact Engineering, 25(3), 253-279.

14. Cantwell, W. J., & Morton, J. (1991). The impact resistance of composite materials—a review. Composites, 22(5), 347-362.
15. Vlot, A., & Gunnink, J. W. (2001). Fibre Metal Laminates: Introductory Notes on Advanced Structural Materials. Springer Science & Business Media.